JEAS
JOURNAL OF ENGINEERING AND APPLIED SCIENCES
Journal of Engineering and Applied Sciences, Volume 20, Number 1, June 2022, 643 - 656

Optimization of Lithium-ion Cell Positive Electrode for Maximization of Energy Capacity

Fidelis N. Okonkwo[1], Chika A. Okonkwo[2], Solomon C. Nwigbo[3],

[1]Department of Mechanical Engineering, Nnamdi Azikiwe University, Awka, Nigeria
[2]Department of Chemical Engineering, Nnamdi Azikiwe University, Awka, Nigeria
[3]Department of Mechanical Engineering, Nnamdi Azikiwe University, Awka, Nigeria
*Corresponding Author's E-mail: fidelfocus@yahoo.com

Abstract
Design expert software is employed for optimization of significant electrochemical materials to enhance low energy capacity of lithium-ion cell that operates variety of consumer electronics devices, electric vehicles and energy storage systems. The design expert experiment, particularly the response methodology effectively explored the variable percentage weight ratio of cathode electrode material composition for adaptability between the predicted and actual experiments. The three optimized samples parameters in the ratio of active material, conductive additive and binder demonstrated significant outputs. Cell sample C with a composition ratio, 92:5:3 displays maximum capacity with high efficiency of design expert response methodology. The outstanding responses from various runs implies substantial effect on the response by each of the factors. The ANOVA analysis and model fitting result indicates non-significant lack of fit. The increment in the percentage weight of binder and active material improves the battery capacity. All the optimized parameters of the three samples have results closely in agreement with the experimental maximum capacity. The compatibility of the responses and analysis implies that the Design expert software is promising for optimization expedient for enhancement of energy capacity of lithium-ion cells.

Keywords: Lithium-ion cell; Design expert; Optimization; Capacity

Abbreviations

NMC: Nickel Manganese Cobalt

CB: Carbon Black

CNTs: Carbon Nanotubes

PVDF: Polyvinylidene Fluoride

FEP: Fluorinated Ethylene Propylene

AM: Active Material

B: Binder

CA: Conductive Additive

1. Introduction

Optimization attempts in the cell industry particularly focus on formulation and modification of electrode composition and structure. Having the knowledge of different stages of mixing in addition to crucial underlying interfacial and surface phenomena offers a long-lasting tool that can lead to superior product quality and reproducibility. The mixing process parameters can be optimized by initiating interrelationship between mixing parameters, slurry material characteristics, finished battery performance and durability (Mohanad, 2017).

Two approaches are to be considered when discussing optimization; sequential and simultaneous. When model is continuously solved within an optimizer, sequential framework is an easy framework to comprehend optimization. Researchers have studied various algorithms that do not require gradient calculations in order to overcome the disadvantages of gradient based optimization (Hare et al, 2018; Gong et al, 2017; Sigmund, 2018). Another sequential approximate technique that can be applied successfully to nonlinear problems without gradient calculation is the so-called progressive quadratic response surface method (Jacobs et al, 2018). Furthermore, the progressive quadratic response surface method requires hardly any calculations for best results, unlike parametric study utilizing a Ragone plot, which needs numerous simulations to analyze a cell (Hong et al, 2016; Alexandrov, 2017; PIDOTECH, 2014). Irrespective of the advantages of progressive quadratic response surface method, it has not been applied to the optimization of lithium-ion cell despite its numerous applications in engineering discipline (Choi et al, 2017; Choi et al, 2016). Simultaneous optimization is feasible with benefits as regards computational performance. Although setting up of sequential approach is much simple when comprehensive models are involved (Suresh & Rengaswamy, 2019). As a result of high theoretical energy density, lithium-ion batteries are generally used as a rechargeable battery (Jelle et al, 2017; Jin-San et al, 2020; Wang et al, 2016; Du et al, 2016; Gao et al, 2016). The improvements and quests on high-capacity lithium-ion cells are witnessing a rise due to increase demand for energy storage systems, consumer electronics and hybrid electric vehicles (Dong-chan et al, 2020; Venter, 2018; Lu, 2018; Tran, 2016; Scrosati and Garche, 2020; Ding et al, 2019; Thackeray et al, 2018; Parvini & Vahidi, 2015; Chen et al, 2017; Yan et al, 2016; Wu et al, 2017).

The energy capacity of these cells must be enhanced in order to cater for this surge. Many researchers are recently conducting studies on the development of new electrode materials, and this requires a reasonable time and effort. Consequently, a good means of reducing the cost of research and development is through optimization of existing electrode material parameters for the enhancement of lithium-ion cell capacity (Ramadesigan, 2016; Doyle et al, 2017; Doyle, 2016; Srinivan & Newman, 2018; Christensena et al, 2016; Stewart et al, 2018; Appiah et al, 2016, Xue, 2018, Golmon et al, 2017; Liu & Liu, 2016). Due to the fact that capacity and power have common relationship, it is important to optimize the design parameters to attain target performance. Nevertheless, collaboration between design parameters and lithium-ion cells performance is extremely non linear (Sang et al, 2015; Chen et al, 2014; Gao et al, 2017). To get rid of this challenge, optimization using design expert surface response methodology is employed. In this study, optimization for the maximum energy capacity of a lithium -ion cell is performed with the aid of design expert software using experimental generated parameters. This paper is structured in 6 sections and a conclusion. The section 1 presents the introductory part, the section 2 presents an overview, the section 3, material and methods, the section 4 presents results and discussions, and section 5 is the conclusion on our results while section 6 is the recommendation.

Battery is an energy storage device consisting of one or more electrochemical cells that produces electrical energy from chemical energy stored in its active materials through electrochemical reactions (Ehsan, 2015). The energy conversion takes place with the aid of electrochemical oxidation-reduction reaction. This type of reactions occurs owing to the transfer of electrons from one type of materials to another via an electric circuit. The energy storage capacity of a battery is the amount of charge that the battery can store/provide at a rated voltage. A battery comprises anode, cathode, and electrolyte as major constituents with separator and current collector as auxiliary components (Surendra, 2017)

Currently, standard lithium-ion battery cathode electrode slurry consists of three components: an active material (60–95%), a binder (2–25%), and conductive additives (3–30%) (Medvedev et al, 2020). The greater number of researchers use the weight ratio of 80%:10%:10% for high-power applications of lithium-ion battery (Goren et al, 2015). In a theoretical study, it was obvious that a binder and carbon black ratio of less than 4 attains the best lithium-ion performance, and the most favourable ratio is 90% of the active material; a binder and conductive additives (carbon black) are from 2 to 8% (Miranda et al, 2019). The ratio of the latter is chosen based on the battery types and conditions of application. Presently, perspective conductive additives such as carbon nanotubes, grapheme and other electrically conductive binder are extensively studied (Sheng et al, 2014). Every one of the above components permits to increase the weight content of the active material, without jeopardizing the conductive properties.

Various studies have been devoted to materials innovation; outstanding achievement has been made as well on the engineering part. The motivation for enhancing electrode production focuses mainly in the potential to notably improves the weight ratio of active materials in lithium-ion batteries, generating higher energy density and lower cost (Li et al, 2017). The electrode components of lithium-ion battery which comprise the active material, binder and

conductive additive give rise to the energy and capacity, electronic conductivity and mechanical strength of the electrode (Blake & Jianlin, 2018). The optimal combination of features between constituents regarding the weight ratios is very crucial (Zheng et al, 2012). The stability and processability of the slurry are the main important properties of a feasible cathode electrode. Knowing that electrode slurry comprises active particles which are considerably bigger than molecules containing the solvent which are reactive to Brownian motion (Mewis & Wagner, 2012). The strength of a cathode electrode slurry is measured by its capacity to withstand agglomeration and sedimentation (Blake & Jianlin).

Response Surface Methodology is a collection of statistical and mathematical techniques which are utilized for setting up a series of experiments for adequate response, fitting a hypothesized model to data generated under the selected experiment (design), determining optimum conditions on the model's input variables that provides maximum or minimum response within an area of interest (Andre, 2017). Kama et al, 2021 studied optimization of culture conditions by response surface methodology for production of extracellular esterase from Serratia. Plackett -Burman design was utilized to determine the effect of six parameters cotton seed oil, peptone and maltose concentrations, PH, temperature and inoculum volume for production of esterase. Four factors; inoculum size, PH, peptone concentration and cotton seed oil concentration had significant effect on production of esterase as suggested by the Pareto chart. The maximum esterase yield was 9.77 U/ml under optimized state with inoculum size (1.0%, v/v), PH (8.0), peptone concentration (1.5%, w/v) and cotton seed oil concentration (4.0%, v/v). analysis of variance (ANOVA) of the central composite design (CCD) based experiment displayed the model F-value of 44.24 and P-value of <0.0001 which implies that the model was significant and adequate to represent the system.

Fan et al, 2012 studied response surface optimization for process parameters of $LiFePO_4$/C preparation by carbothermal reduction technology. The experimental data for fitting the response are obtained by the central composite design. A second order model for the discharge capacity of $LiFePO_4$/C is demonstrated as a function of sintering temperature, sintering time and carbon content. The outcome of each variable and their interactions are studied by ANOVA analysis. The result show that the linear and quadratic effect of carbon content, sintering temperature and interactions among these variables are statistically significant while those effects of sintering time are insignificant. The P-value greater than 0.1 indicates non-significant model terms whereas value less than 0.0500 indicates significant model terms. The small P-value (<0.0001) and large F-value (=94.7) implies significant quadratic model.

2. Material and Methods

2.1 Material

The active material, the binder and conductive additive are the cathode electrode control factors due to the characteristics of the composite elements as follows;

Nickel; it assists to deliver high energy density to the composites and it offers greater storage capacity at a cheap cost.

Manganese; It forms a spinel structure to achieve low internal resistance, offers low specific energy and provides cycle stability to the active material structure.

Cobalt; It enhances the rate performance of a cell, aids batteries to accept lithium ions at a high rate during charging and deliver lithium ions at a high rate during discharge (Audi et al, 2017).

Polyvinylidene fluoride (PVDF); Chemical inertness and dual function, it can be used in both negative and positive electrode formulations.

Fluorinated ethylene propylene (FEP); It has good dielectric strength, flexible mechanical strength and thermally stable

Carbon Black (CB); Channel black is a good choice for higher battery stability and high voltage (Morfeld & McCunney 2007). It also provides higher battery capacity and rate capability with light weight

Carbon Nanotubes (CNTs); It exhibit remarkable electrical conductivity (Bever et al, 2010)

They have exceptional tensile strength and thermal conductivity due to their nanostructure and strength of the bonds between carbon atoms (Yu et al, 2010)

2.2 Methods

The weight ratio of active material (NMC) to binder (PVDF+FEP) and conductive additive (CB+CNTs) is 94:3:3 weight % for sample A, 90:5:5 weight % and 92:5:3 weight % for sample B and C respectively. The cathode electrode materials were sourced from Soundon Energy Ltd, China while the fabrication and experimental analysis were carried out by Benzo Technology, China. The knowledge obtained from the literatures was applied in determining the

percentage weight ratios. The conductive additive and binder were dried in a vacuum oven for 24 hours before use, the binder was dissolved in the solvent *N*-Methyl-2-pyrrolidone (NMP) in a planetary mixer de-aerator (SWXJ-SOWER) operated at 670 rpm rotation and 1130 rpm revolution with a total time of 6 minutes. Thereafter the conductive additive was added to the binder solution followed by mixing at 4000 rpm for 45 minutes in a homogenizer (Konmix, KRH-75). Thirdly, the active material (NMC) was added to the homogenizer, and the mixture was mixed at 4000 rpm for 1 hour. Finally, the homogeneous slurry was placed in a vacuum chamber for 5 minutes to remove any trapped bubbles and thereafter removed out of the chamber to cast at room temperature onto 15 μm thick aluminum foil with an automatic compact film coater which has an in-built dryer and vacuum chuck (Benzo Technology). For casting, the adjustable doctor blade gap was set at 200 μm and the casting speed was 0.15 m/30s.

Applying the Immersion precipitation method for membrane fabrication, the cast electrode was instantly immersed in a de-ionized water bath at 25°C for 120s followed by a pre-drying step by exposing the electrode in dry air for 5 minutes. The electrodes were dried at room temperature overnight. The electrode was calendared with a 40 μm rolling gap using a compact electric rolling press (Gn-Gy-150) at room temperature to improve the adhesion of the compatible electrode materials with the Al foil, and control the porosity and packing density (Sheng et al, 2014). The calendered electrode was punched to a specified dimension with a Precision pouch punching mould (Benzo Technology) and further dried in vacuum oven for 12 hours at 130°C. For comparison, positive cathode electrodes of varying compositions for the three different cell samples were prepared by the same method using the same mixing sequence and parameters.

Table 3.1 Positive Electrode Fabrication Data

Sample	**NMC (%) Ratio**	**AM:B:CA (%) Ratio**	**B:CA (%) Ratio**	**Sample (mm) Dimension**
A	0.4:0.3:0.3	94:3:3	1:1	48x30x7
B	0.3:0.3:0.3	90:5:5	1:1	60x50x6
C	0.5:0.3:0.2	92:5:3	1:0.6	60x50x8

Table 3.2 Cell Sample A Basic Performance Test Data

No	**Item**	**Parameter**	**Note**
1.	Maximum Capacity	1200 mAh	Fully discharged (0.2C C_5A) after fully charged.
2.	Nominal Capacity	1000 mAh	
3.	Maximum Cell Initial Impedance	165 mΩ	3.7V AC 1KHz
4.	Nominal Voltage	3.7 V	Mean Operation Voltage
5.	Initial Voltage	3.75 V	
6.	Limited Charge Voltage	4.2 V	Voltage of CC charge to CV charge
7.	Cut-off Voltage	2.75 V	Discharge Cut-off Voltage.
8.	Open-Circuit Voltage	4.06V	To be measured within 24 hours after fully charged.
9.	Nominal Energy	3.7Wh	
10.	Charging Current	240 mA (0.2C)	
11.	Discharging Current	240 mA (0.2C)	
12.	Maximum Discharge Current	1200 mA (1.0C)	
13.	Charging Time	5 hours	Maximum
14.	Rapid Charging Time	2 hours	Maximum

Table 3.3 Cell Sample B Basic Performance Test Data

No	**Item**	**Parameter**	**Note**
1.	Maximum Capacity	2100 mAh	Fully discharged (0.2C C_5A) after fully charged.
2.	Nominal Capacity	2000 mAh	
3.	Maximum Cell Initial Impedance	160 mΩ	3.7V AC 1KHz
4.	Nominal Voltage	3.7 V	Mean Operation Voltage
5.	Initial Voltage	3.75 V	
6.	Limited Charge Voltage	4.2 V	Voltage of CC charge to CV charge

7.	Cut-off Voltage	2.75 V	Discharge Cut-off Voltage.
8.	Open-Circuit Voltage	4.07V	To be measured within 24 hours after fully charged.
9.	Nominal Energy	7.4Wh	
10.	Charging Current	240 mA (0.2C)	
11.	Discharging Current	240 mA (0.2C)	
12.	Maximum Discharge Current	2100 mA (1.0C)	
13.	Charging Time	Approx. 6 hours	Maximum
14.	Rapid Charging Time	Approx. 3 hours	Maximum

Table 3.4 Cell Sample C Basic Performance Test Data

No	Item	Parameter	Note
1.	Maximum Capacity	3100 mAh	Fully discharged (0.2C C_5A)
2.	Nominal Capacity	3000 mAh	after fully charged.
3.	Maximum Cell Initial Impedance	150 mΩ	3.7V AC 1KHz
4.	Nominal Voltage	3.7 V	Mean Operation Voltage
5.	Initial Voltage	3.75 V	
6.	Limited Charge Voltage	4.2 V	Voltage of CC charge to CV charge
7.	Cut-off Voltage	2.75 V	Discharge Cut-off Voltage.
8.	Open-Circuit Voltage	4.08V	To be measured within 24 hours after fully charged.
9.	Nominal Energy	11.1Wh	
10.	Charging Current	240 mA (0.2C)	
11.	Discharging Current	240 mA (0.2C)	
12.	Maximum Discharge Current	3100 mA (1.0C)	
13.	Charging Time	Approx. 6 hours	Maximum
14.	Rapid Charging Time	Approx. 3 hours	Maximum

3.0 Results and Discussions

3.1 Optimization of the Composite Materials

The response obtained from the experimental runs carried out by combinations of the three variables (active material, binder and conductive additive) are shown on the response column of Table 4.1. The three experimental variables interaction generate a total of 20 experimental runs. The responses obtained from various runs were significantly outstanding which implies that each of the factors have substantial effect on the response.

3.2 ANOVA Analysis and Model Fitting

The Model F-value of 49.60 implies the model is significant. There is only an 0.01% chance that an F-value this large could occur due to noise. Values of "Prob > F" less than 0.0500 indicate model terms are significant. In this case A, B, C, BC, A^2, B^2, C^2 are significant model terms. Values greater than 0.1000 indicate the model terms are not significant. The adequacy of the model was evaluated by applying lack of fit test as shown in Table 4.2. The test for lack of fit compares variation around the model with pure variation within repeated observations. This test measures the adequacy of different models based on response surface analysis (Lee et al, 2006). Non-significant lack of fit is desirable because it implies the model will produce a good fit. Hence, the ANOVA and lack of fit validates the generated model. In comparison with the research of Kama et al, 2021 as presented in the literature, the obtained ANOVA results are in communion, which are adequate for the system.

3.3 Effect of actual and predicted values

The response values obtained by inserting the independent values are the predicted values of the model. These values are compared to the actual experimental values. The result of this comparison is shown in Figures 4.1a, 4.1b, 4.1c and 4.1d respectively. The linear correlation for the cell samples represents a confidently distributed relationship between

the predicted and actual values which is attributed to the improved material composite, due to the experimental approach.

Table 4.1: Factors and Response

		Factor 1	Factor 2	Factor 3	Response 1
Std	Run	A:Active material %	B:Binder %	C:Conductive additive %	Capacity mAh
1	5	90.8	3	3	1500
2	15	93.2	3	3	2400
3	19	90.8	5	3	2900
4	8	93.2	5	3	3200
5	10	90.8	3	5	900
6	1	93.2	3	5	1000
7	9	90.8	5	5	1100
8	12	93.2	5	5	1900
9	20	90	4	4	1200
10	17	94	4	4	2100
11	11	92	2.3	4	1400
12	6	92	5.7	4	3100
13	2	92	4	2.3	3100
14	18	92	4	5.7	1000
15	14	92	4	4	2600
16	13	92	4	4	2600
17	7	92	4	4	2600
18	3	92	4	4	2600
19	4	92	4	4	2600
20	16	92	4	4	2600

Table 4.2: ANOVA for Response Surface Quadratic Model Analysis of variance table [Partial sum of squares - Type III]

Source	Sum of Squares	df	Mean Square	F Value	p-value Prob > F
Model	1.173E+007	9	1.303E+006	49.60	< 0.0001
A-Active material	9.562E+005	1	9.562E+005	36.39	0.0001
B-Binder	2.778E+006	1	2.778E+006	105.72	< 0.0001
C-Conductive additive	5.456E+006	1	5.456E+006	207.64	< 0.0001
AB	1250.00	1	1250.00	0.048	0.8317
AC	11250.00	1	11250.00	0.43	0.5276
BC	1.513E+005	1	1.513E+005	5.76	0.0374
A^2	1.801E+006	1	1.801E+006	68.53	< 0.0001
B^2	2.879E+005	1	2.879E+005	10.96	0.0079
C^2	6.481E+005	1	6.481E+005	24.67	0.0006
Residual	2.627E+005	10	26274.45		
Lack of Fit	2.627E+005	5	52548.90		
Pure Error	0.000	5	0.000		
Cor Total	1.199E+007	19			

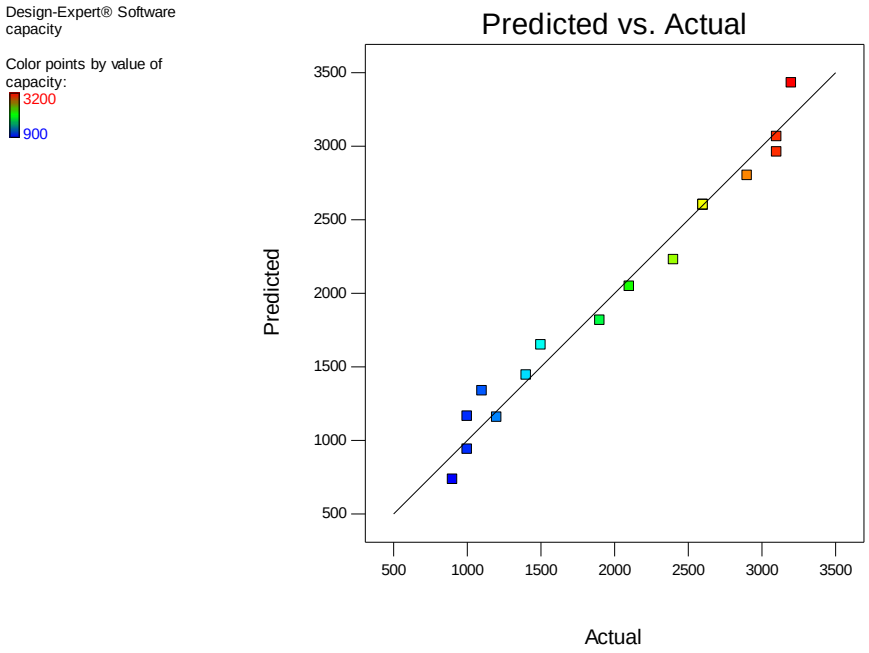

Figure 4.1 (a) Correlation between predicted vs actual values for the cell samples

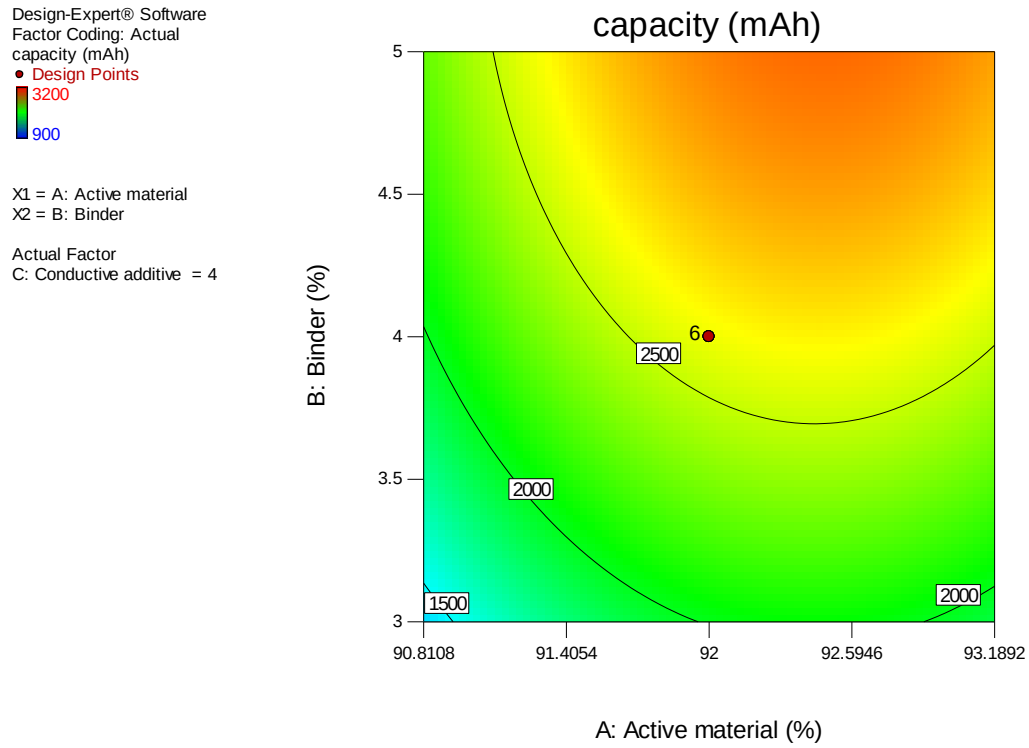

Figure 4.1 (b) double effect plot for the effect of binder and active material on the cell capacity

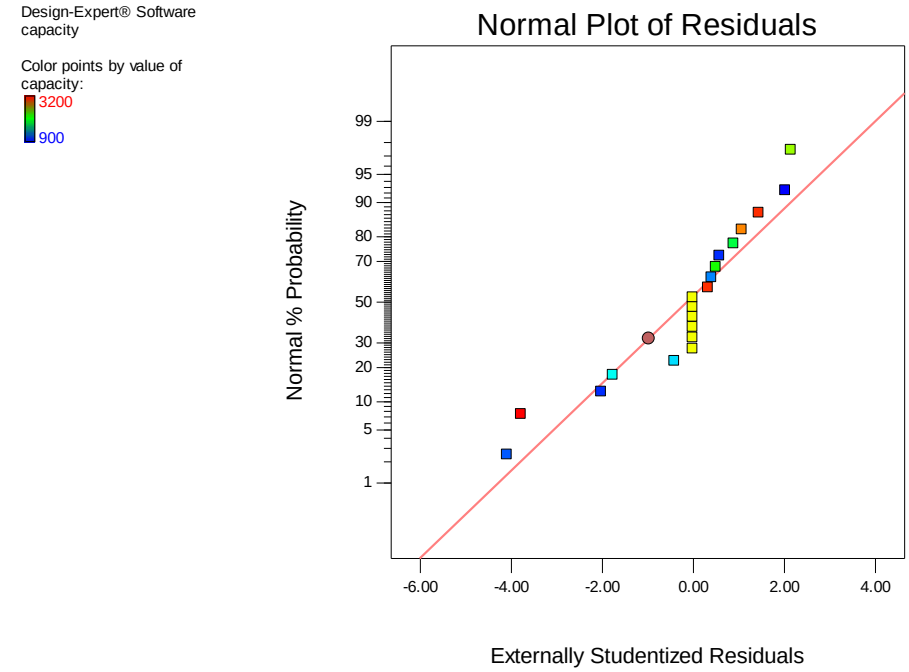

Figure 4.1 (c) Correlation between normal plot of residuals and normal % probability

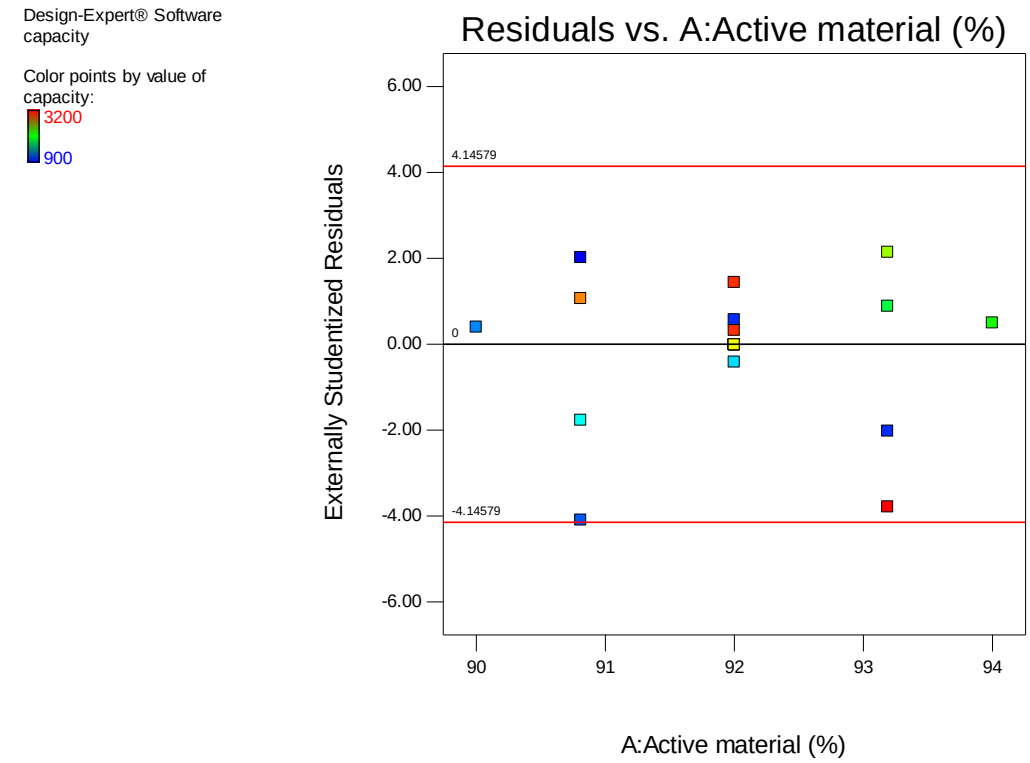

Figure 4.1 (d) Correlation between residuals and active material

4.4 Effect of composite parameters

The graph of binder versus active material indicates increment in the percentage of binder and that of active material, which increases the battery capacity (Figure 4.2a). The graph of conductive additive versus active material indicates negative effect of conductive additive on the cell capacity, which decreases the capacity whereas increment in the active material gives positive result to the cell capacity, which increases the capacity (Figure 4.2b). The graph of conductive additive versus binder also indicates negative effect of conductive additive on the cell capacity, which decreases the capacity while binder provides positive result on the capacity, which increases the capacity (Figure 4.2c).

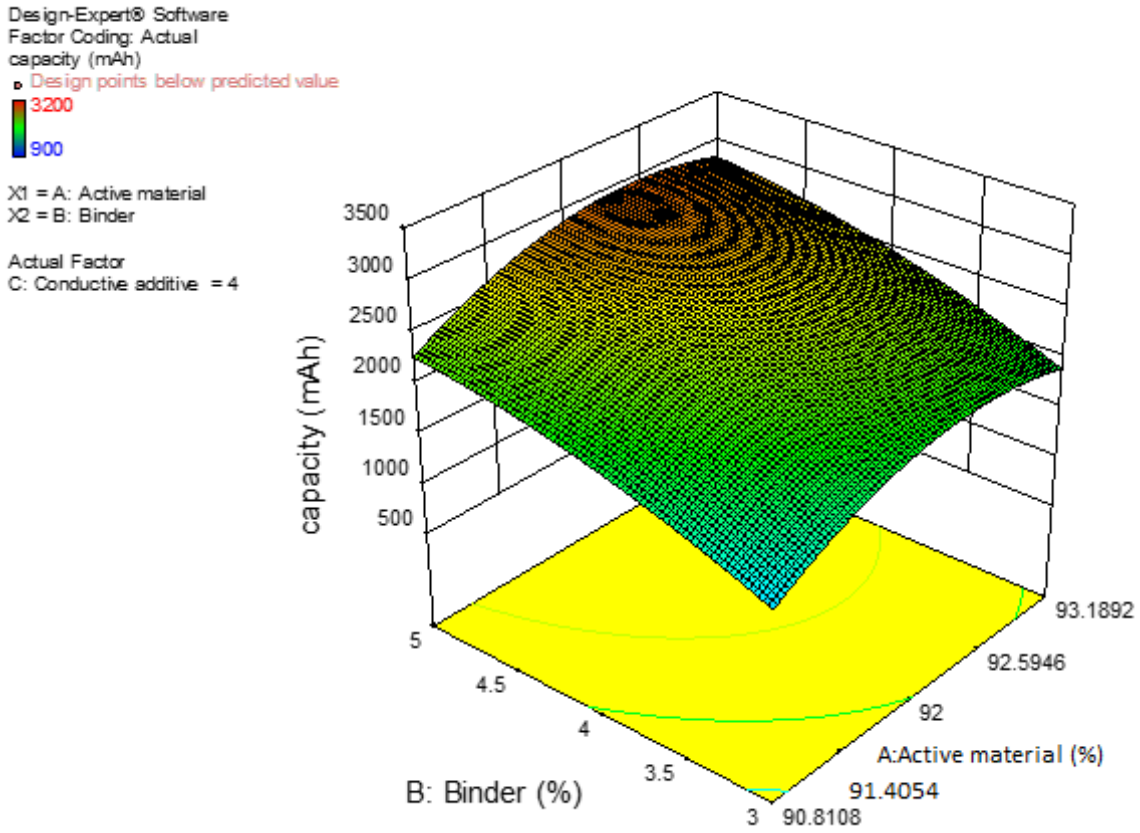

Figure 4.2 (a) 3D surface plot for the effect of active material and binder on the cell capacity

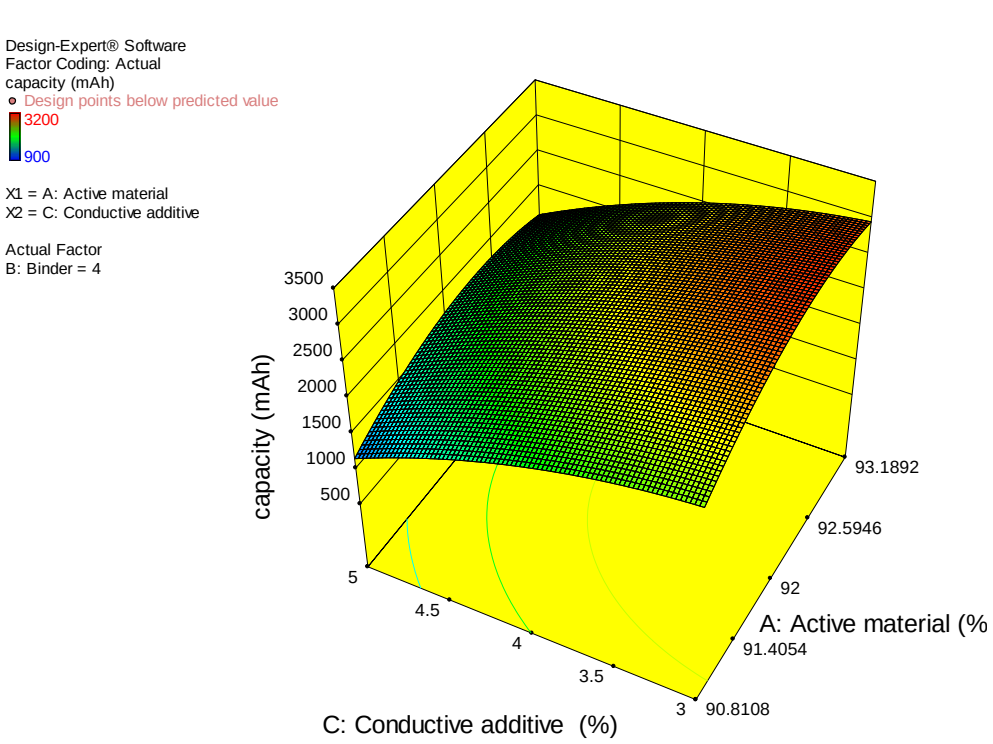

Figure 4.2 (b) 3D surface plot for the effect of active material and conductive additive on the cell capacity

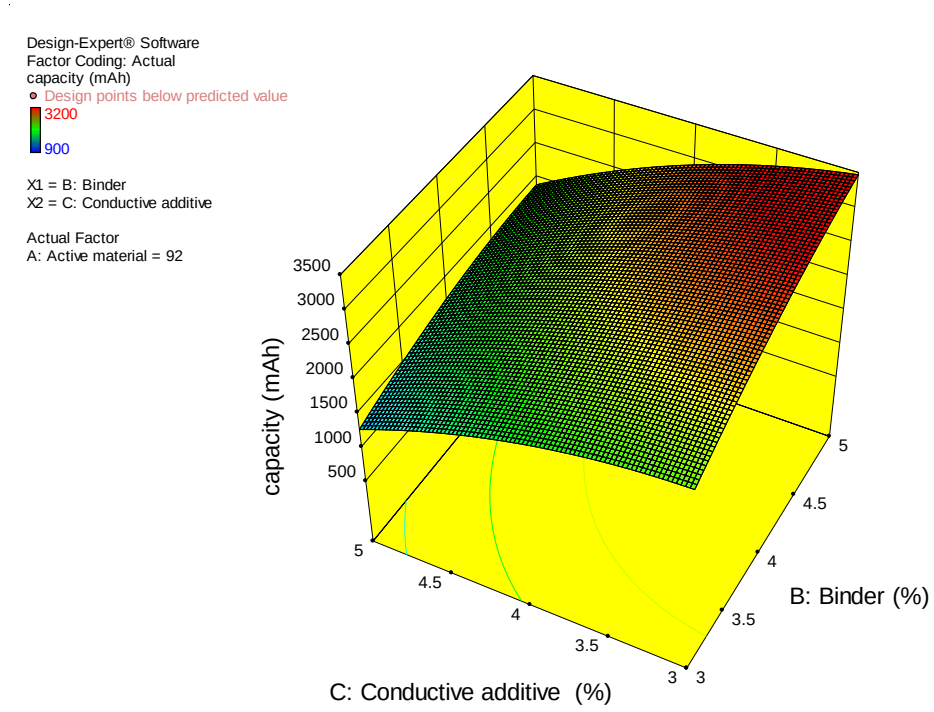

Figure 4.2 (c) 3D surface plot for the effect of conductive additive and binder on the cell capacity

4.5 Optimization

Position seven (7) of the table was preferred as the optimized composition against selected position one (1) Table 4.3. This is because the solution at that position conforms with the result of the graph(s), which indicates that increment in the percentage weight of the binder and that of active material, increases the cell capacity. Additionally, the generated maximum optimized capacity occurs at that position, which is approximately the same as the experimental maximum capacity.

Table 4.3 Optimization of the composite materials

Name	Goal	Lower Limit	Upper Limit	Lower Weight	Upper Weight	Importance
A:Active material	is in range	90.8	93.2	1	1	3
B:Binder	is in range	3	5	1	1	3
C:Conductive additive	is in range	3	5	1	1	3
Capacity	none	900	3200	1	1	3

Table 4.4 Optimum solution for the composite materials

Number	Active material	Binder	Conductive additive	capacity	Desirability	
1	92.294	4.088	4.879	1947.652	1.000	Selected
2	93.189	3.000	3.000	2228.966	1.000	
3	92.000	4.000	4.000	2602.694	1.000	
4	90.811	3.000	3.000	1649.765	1.000	
5	90.811	5.000	5.000	1337.644	1.000	
6	90.811	3.000	5.000	735.672	1.000	
*7	93.189	5.000	3.000	3430.938	1.000	Preferred
8	93.189	5.000	5.000	1816.845	1.000	
9	93.189	3.000	5.000	1164.874	1.000	
10	93.144	3.961	3.994	2515.621	1.000	

5.0. Conclusion

Optimization of lithium-ion cell positive electrode for maximization of energy capacity, successfully performed using design expert software presented significant throughput. The optimized capacity, cell initial impedance, nominal voltage, cut-off voltage, nominal energy, charging/discharging current, charging time, etc. were performed concurrently across the model samples. Evidence, design expert experiment demonstrating these optimization factors, as repeatedly performed data displays high degree of adaptability between the predicted and actual experiments. Thus, the active material, which contributes to 90 % capacitance of lithium-ion storage, shows consistent improved average energy capacity in the range of 1,500 – 3,200 mAh. Adequacy of the model further showed, as demonstrated with ANOVA analysis by evaluating the lack of fit test, consistent model F-value of 49.60 known for significant model. In fact, the three experimental variables interaction generated a total of 20 experimental runs with close margin response, suggesting sustainable design expert application. These composites used for the experiment also demonstrated the proportion ratio of active material to binder, 94:3 with superior energy capacity. The results shows that design expert surface methodology-based optimization is promising for designing experiments with NMC and similar related materials would be successfully optimized.

6.0 Recommendation

The main focus of this study was to maximize the energy capacity of lithium-ion cells using Design expert surface methodology. The existing framework can be developed to enhance the real effect of the optimization results by attempting various views. At first, comprehensive micro-structure modeling can be integrated into the cell model to give accurate cell design optimization. Furthermore, a multi-point optimal design can be ascertained by utilizing an aggregate objective function.

References

Alexandrov, N., 2017. Robustness properties of a trust region framework for managing approximations in engineering optimization. https://doi.org/10.2514/6.1996-4102.

Andre., 2017. general overview of response surface methodology. Department of Statistics, University of Florida, USA

Audi, G., Kondev, F. G, Wang, M, Huang, W. J & Naimi, S. 2017. "The NUBASE2016 evaluation of nuclear properties" (PDF). *Chinese Physics C*. 41 (3): 030001.

Appiah, W.A., Park, J., Song, S., Byun, S., Ryou, M.H., & Lee, Y.M, 2016. Design optimization of LiNi0.6Co0.2Mn0.2O2/graphite lithium-ion cells based on simulation and experimental data. *J. Power Sources*. 1:2–3. https ://doi.org/10.1016/j.jpowersource.2016.04.052.

Bever, S.; Kwon, Y. K & Tomanek, D. 2010.. "Unusually high thermal conductivity of carbon nanotubes". Phys. Rev. Lett. 84: 4613–4616.

Blake, W. H & Jianlin, L. 2018 Electrode Manufacturing for Lithium-Ion Batteries – Analysis of 1 Current and Next Generation Processing. Oak Ridge National Laboratory, Energy and Transportation Science Division, Oak Ridge, TN, USA 37831

Chen, Z., Shu, X., & Sun, M., 2017. Charging strategy design of lithium-ion batteries for energy loss minimization based on minimum principle[C].*IEEE Transportation Electrification Conference and Expo, Asia-Pacific.* IEEE, 2017:1-6.

Chen, Z., Xia, B., & Mi, C. C., 2014. Loss minimization-based charging strategy for lithium-ion battery[C].*Energy Conversion Congress and Exposition*. IEEE, 2014:4306-4312.

Christensena, J., Srinivasan, V., & Newman, J., 2016. Optimization of lithium titanate electrodes for high-power cells. *J. Electrochem. Soc.* https ://doi.org/10.1149/1.21725 35 (2016).

Ding, Y., Cano, Z. P., Yu, A., Lu, J., & Chen, Z., 2019. Automotive li-ion batteries: Current status and future perspectives. *Electrochem. Energy Rev*. https ://doi.org/10.1007/s4191 8-018-0022-z

Dong-chen, L., Kyu-Jin, L., & Chang-Wan, K., 2020. Optimization of a Lithium-Ion Battery for Maximization of Energy Density with Design of Experiments and Micro-genetic Algorithm, *International Journal of Precision Engineering and Manufacturing Green Technology*, Volume 7, Pages 829 – 836.

Doyle, M., Fuller, T. F., & Newman, J., 2017. Modeling of galvanostatic charge and discharge of the lithium polymer insertion cell. *J. Electrochem. Soc*. https ://doi.org/10.1149/1.22215 97.

Doyle, C.M., 2016. Design and Simulation of Lithium Rechargeable Batteries. *Technical Report.* https ://escho larsh ip.org/conte nt/qt6j8 7z0sp /qt6j8 7z0sp .pdf.

Choi, J. H., Kim, T. H., Jang, K. B., & Lee, J., 2003. Geometric and electrical optimization design of SR motor based on progressive quadratic response surface method. *IEEE Trans. Magn.* https ://doi.org/10.1109/TMAG.2003.81673 4.

Choi, H. I., Lee, Y., Choi, D. H., Maeng & J. S., 2010. Design optimization of a viscous micropump with two rotating cylinders for maximizing efficiency. *Struct Multidiscip. Optim*. https ://doi.org/10.1007/s0015 8-009-0373-5.

Du, J., Ouyang, M., & Chen, J., 2017. Prospects for Chinese electric vehicle technologies in 2016–2020: *Ambition and rationality. Energy* 2017,120, 584–596.

Ehsan, S 2015. Modeling Of Lithium-Ion Battery Performance and Thermal Behavior In
Electrified Vehicles, Mechanical Engineering Department, University of Waterloo, Ontario, Canada.

Fan, W., Yang, K., Tan, F., Long, Y & Wen, Y., 2012. Response Surface Optimization for Process Parameters of LiFePO4/C Preparation by Carbothermal Reduction Technology. *Chinese Journal of Chemical Engineering*, **20**(4) 793-802.

Gao, C., Xie, Q., & Li, Y., 2016. Phased Pulse Charging Method Based on Lithium-ion Power Battery [J]. *Electrical Engineering & Energy Efficient Management Technology*, 2016(18):50-55.

Gao, Y., Jiang, J., & Zhang, C., 2017. *Lithium-ion battery aging mechanisms and life model under different charging stresses* [J].*Journal of Power Sources*, 2017, 356.

Golmon, S., Maute, K., & Dunn, M. L., 2017. Multiscale design optimization of lithium-ion batteries using adjoint sensitivity analysis. *Numer. Methods Eng.* https ://doi.org/ 10.1002/ nme. 4347.

Gong, J. X., Yi, P. & Zhao, N. 2017 Non-gradient–based algorithm for structural reliability analysis. *J. Eng. Mech.* https ://doi.org/10.1061/ (ASCE)EM.1943-7889.00007 22.

Goren, A., Costa, C. M., Silva, M. M & Lanceros-Mendez, S. 2015. State of the art and open questions on cathode preparation based on carbon coated lithium iron phosphate. Compos B 83:333–345. https://doi.org/10.1016/j.compositesb.2015.08.064

Hare, W., Nutini, J., & Tesfamariam, S., 2018. A survey of non-gradient optimization methods in structural engineering. *Adv. Eng. Softw*. https ://doi.org/10.1016/j.adven gsoft .2018.03.001.

Hong, K. J., Kim, M. S., & Choi, D. H., 2016. Efficient approximation method for constructing quadratic response surface model. *KSME Int. J*. https ://doi.org/10.1007/BF031 85266.

Jacobs, J. H., Etman, L. F. P., Van Keulen, F., & Rooda, J. E., 2018. Framework for sequential approximate optimization. *Struct. Multidiscip. Optim*. https ://doi.org/10.1007/s0015 8-004-0398-8.

Jelle, S., Noshin, O., Annick, H., Joeri, V.M. & Peter, V.B., 2017. *Optimization of Li-Ion batteries through modelling techniques.* Erasmus University College Brussels, IWT Nijver heidskaai 170, 1070 Anderlacht Belgium EVS28.

Kama, K.B., Rakesh, K., Suhani., B & Reena, G., 2021. Optimization of culture conditions by response surface methodology for production of extracellular esterase from Serratia. *Journal of king saud university.* Science 33 (2021) 101603.

Li, J., Du, Z., Ruther, R. E., David, L. A., Hays., K & Wood, M. 2017. Toward Low-Cost, High-Energy Density, and High-Power Density Lithium-Ion Batteries, JOM 69; 1484-1496. https://doi.org/10.1007/s11837-017-2404-9.

Liu, C. & Liu, L. 2016. Improving battery safety for electric vehicles through the optimization of battery design parameters. *J. Electrochem. Soc.* https ://doi.org/10.1149/06920 .0005e cst.

Lu, W. 2018. High-energy electrode investigation for plug-in hybrid electric vehicles. *Journal of Power Sources*,196, 1537–1540.

Ji-San, K., Dong-Chan, L., Jeong-Joo, L. & Chang-Wan, K., 2020. Optimization for maximum specific energy density of a lithium-ion battery using progressive quadratic response surface method and design of experiments. *Scientific Reports, natureresearch*. (2020) 10:15586.

Medvedev, O. S., Wang, O., Popovich, A. A & Novikov, P. A. 2020. Comparison of conductive additives for high-power applications of Li-ion batteries. Ionics. Vol. 26; 4277-4286

Mewis, J & Wagner, N. 2012. Colloidal Suspension Rheology, first ed., Cambridge University Press, Cambridge

Miranda, B., Goren, A & Costa, C. M 2019. Theoretical simulation of the optimal relation between active material, binder and conductive additive for lithium-ion battery cathodes. Energy 172:68–78. https://doi.org/10.1016/j.energy.2019.01.122\

Mohanad, N. A., 2017. Chemical and Materials Engineering, University of Kentucky. https://doi.org/10.13023/ETD.2017.296.

Morfeld., P & McCunney., R.J 2007. "Carbon black and lung cancer: Testing a new exposure metric in a German cohort". *Am J Ind Med*. 50 (8): 565–567. doi:10.1002/ajim.20491. PMID 17620319.

Parvini, Y & Vahidi, A. 2015. Maximizing charging efficiency of lithium-ion and lead-acid batteries using optimal control theory[C]. *American Control Conference. IEEE*, 2015:317-322.

PIDOTECH, 2014. PIAnO User's Manual, *PIDOTECH Inc.*, (2014).

Ramadesigan, V. 2016. Modeling and simulation of lithium-ion batteries from a systems engineering perspective. *J. Electrochem. Soc*. https ://doi.org/10.1149/2.01820 3jes (2016).

Sang, K.M., Sun, L., & Chan, W.L. 2015 Identification and modelling of Lithium-ion battery. *Energy Convers Manag*.2015, 51, 2857–2862.

Scrosati, B., & Garche, J. 2020. Lithium batteries: Status, prospects and future. *Journal of Power Sources,195*(9), 2419–2430.

Sheng, Y., Fell, C.R., Son, Y.K., Metz, B.M., Jiang, J & Church, B.C., 2014. 'Effect of Calendering on Electrode Wettability in Lithium-Ion Batteries', *Frontiers in Energy Research*, 2, p. 56.

Sigmund, O. 2018. On the usefulness of non-gradient approaches in topology optimization. *Struct. Multidiscip. Optim.* https ://doi. org/10.1007/s0015 8-011-0638-7 (2018).

Srinivasan, V. & Newman, J. 2018. Design and optimization of a natural graphite/iron phosphate lithium-ion cell. *J. Electrochem. Soc.* https ://doi.org/10.1149/1.17850 13 (2018).

Stewart, S. G., Srinivasan, V. & Newman, J. 2018. Modeling the performance of lithium-ion batteries and capacitors during hybrid electric- vehicle operation. *J. Electrochem. Society*. https ://doi.org/10.1149/1.29535 24 (2018).

Surendra, B. 2017 Mathematical Modeling And Capacity Fading Study In Porous Current Collector Based Lithium Ion Battery.

Suresh, R. M. P & Rengaswamy, R., 2019. Modeling failure modes in Li-ion battery. *AIChE Annu. Meet.*

Thackeray, M. M., Wolverton, C. & Isaacs, E. D. 2018. Electrical energy storage for transportation. Approaching the limits of, and going beyond, lithium-ion batteries. *Energy Environ. Sci.* https ://doi.org/10.1039/C2EE2 1892E (2018).

Tran, H. Y. 2016. Influence of electrode preparation on the electrochemical performance of $LiNi_{0.8}Co_{0.15}Al_{0.05}O_2$ composite electrodes for lithium-ion batteries. *Journal of Power Sources,210,* 276–285.

Venter, G. 2018. Review of optimization techniques encyclopedia of aerospace engineering. vol 8. New York: Wiley.

Wang, Z., Wang, Y., & Rong, Y., 2016. Study on the Optimal Charging Method for Lithium-Ion Batteries Used in Electric Vehicles [J]. *Energy Procedia*, 2016, 88:1013-1017.

Wu, X., Shi, W., & Du, J., 2017 Multi-Objective Optimal Charging Method for Lithium-Ion Batteries [J]. *Energies*, 2017, 10(9):1271.

Xue, N. 2018 Optimization of a single lithium-ion battery cell with a gradient-based algorithm. *J. Electrochem. Soc.* https ://doi. org/10.1149/2.03630 8jes (2018).

Yan J, Xu G, & Qian H, 2016. Model Predictive Control-Based Fast Charging for Vehicular Batteries[J]. *Energies*, 2016, 4(8):1178-11963390.

Yu, M. F; Lourie, O., Dyer, M.J., Moloni, K., Kelley, T.F & Ruoff, R.S (2010). "Strength and breaking mechanism of multiwalled carbon nanotubes under tensile load". Science. 287 (5453): 637–40.

Zheng, H., Yang, R., Liu, G., Song, X & Battagllia. V. S 2012. Cooperation between Active Material, Polymeric Binder and Conductive Carbon Additive in Lithium Ion Battery Cathode, *J. Phys. Chem. C 116;4875-4882.*